Cause Investigation of Capsizing Accident of Ro-Ro Ferry Ship using Marine Accident Integrated Analysis System

Sang-Gab Lee, Jae-Seok Lee, Ji-Hoon Park and Tae-Young Jung

Korea Maritime & Ocean University, Marine Safety Technology, Busan, Korea

1 Abstract

Ro-Ro ferry ship was capsized and was sunk down to the bottom in the sea water due to the rapid turning for the several reasons, such as lack of stability and poor lashing, etc. Objective of this study is to investigate the capsize accident cause by full-scale ship rapid turning simulation through the comparison with AIS track in this capsize accident, considering several factors, such as GoM, ship velocity, rudder angle, etc., and using Marin Accident Integrated Analysis System (highly advanced M&S system of FSI analysis technology). MAIAS of full-scale ship turning simulation are verified by comparison with maneuvering performance sea trial test result of initial building ship. Several things were carried for this rapid turning simulation, such as accurate ship model modification using floating simulation according to hydrostatic characteristics of loading conditions, and investigation of cargo loading arrangement and cargo lashing states. There was relatively good agreement of full-scale ship sea trial turning simulation with sea trial test result, and good prediction of cargo loading arrangement and cargo lashing states comparing to the AIS track in this capsize accident.

***Keyword Words**: Ro-Ro Ferry Ship; Capsizing Accident; Marine Accident Integrated Analysis System (MAIAS); Highly Advanced Modeling & Simulation (M&S) System; Fluid-Structure Interaction (FSI) Analysis Technique; Full-Scale Ship Rapid Turning Simulation; Floating Simulation; Hydrostatic Characteristics Program.*

2 Introduction

Ro-Ro ferry ship was capsized during rapid turning passing through the east sea of Byeongpungdo island in Jindogun, as shown in Fig. 1, due to the several reasons, such as gravity rise due to excessive extension and rebuilding of stern part, lack of stability with shortage ballast and excessive cargo loading, excessive outward heel due to small GM during rapid turning, and cargo leaning according to lateral heel angle due to poor lashing, etc. Objective of this study is to investigate the cause of capsize accident, analyzing the rudder angle, ship velocity, GM, and cargo lashing at the accident, and carryingout full-scale rapid turning simulation according to its variable using Marine Accident Integrated Analysis System (MAIAS; highly advanced M&S system using FSI analysis technology of LS-DYNA code [1~3]), and comparing its simulation results with the real AIS track and heeling angle. MAIAS was verified through the full-scale ship turning simulation by comparison with maneuvering performance sea trial test result of initial building ship. Several things were carried for this rapid turning simulation, such as accurate ship modeling using floating simulation according to hydrostatic characteristics of loading conditions, and investigation of cargo loading arrangement and cargo lashing states. This study was supported by the gathered research materials by Special Investigation Commission on 4/16 Sewol Ferry Disaster and previous reports[4~6].

Fig.1: Ferri ship capsize accident photo, accident spot, and rapid turning place and depth

3 Full-Scale Ship Modeling

Exact full-scale ship modeling including exterior openings and interior transferring paths was carried for the full-scale turning and flooding simulation using MAIAS, figuring out the lines, general arrangement, construction drawings, etc., as shown in Figs. 2 & 3. Full-scale ship modeling was modified through the validation of its center, buoyance, center of floatation, and each tank volume by carrying out the floating simulation according to loading condition of stability calculation. In addition to the floating simulation, the fore and aft draft and hydrostatic characteristics was also verified using hydrostatic characteristic program. Figure 4 shows the tank layout modeling in the side, top and iso view, and also each tank volume and displacement, fore and aft drafts in the light loading condition.

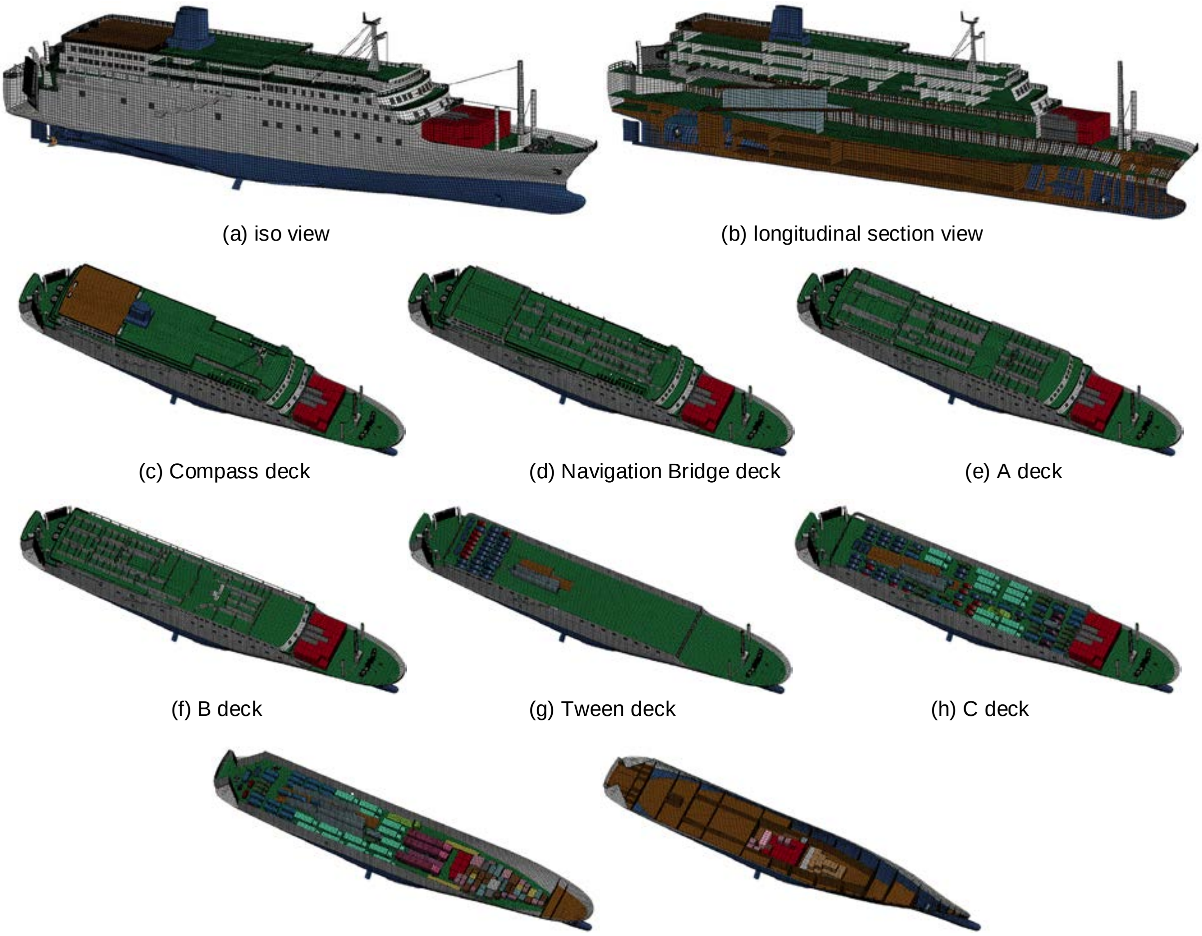

(a) iso view (b) longitudinal section view
(c) Compass deck (d) Navigation Bridge deck (e) A deck
(f) B deck (g) Tween deck (h) C deck
(i) D deck (j) E deck

Fig.2: Full-scale ship model including each deck with cargo

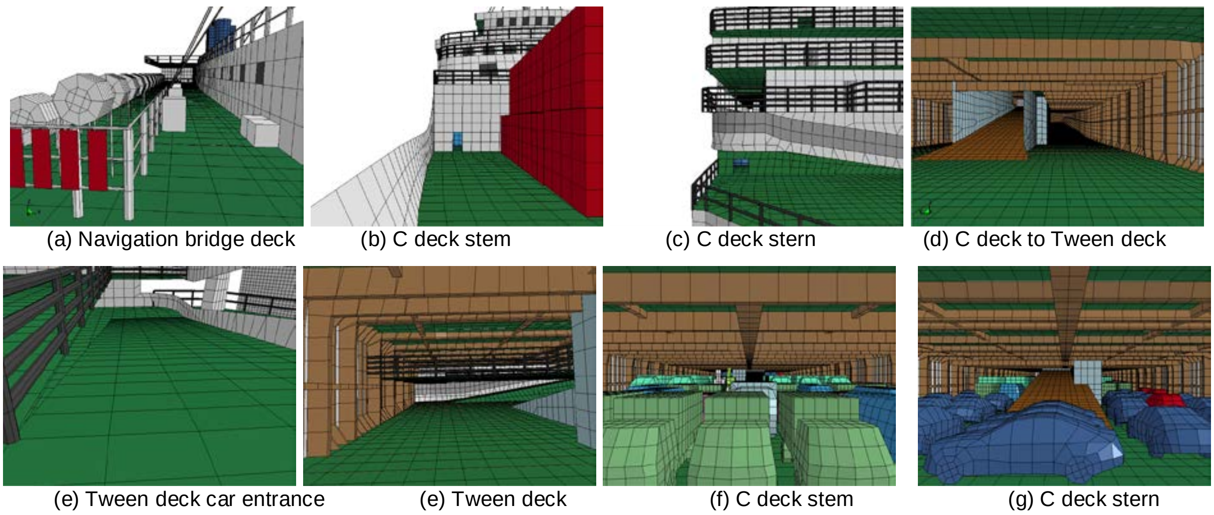

(a) Navigation bridge deck (b) C deck stem (c) C deck stern (d) C deck to Tween deck
(e) Tween deck car entrance (e) Tween deck (f) C deck stem (g) C deck stern

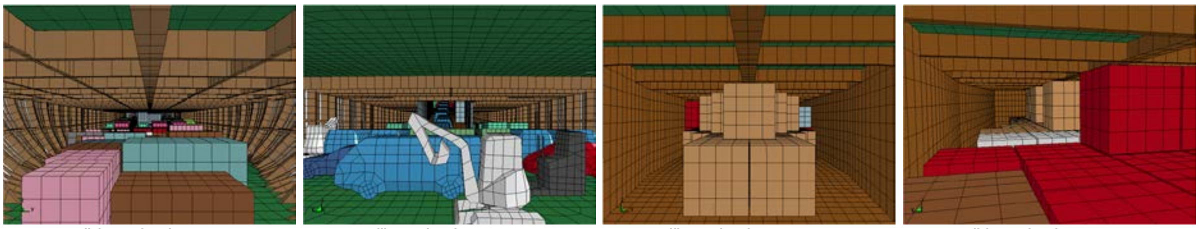

(h) D deck stem (i) D deck stern (j) D deck stem (k) E deck stern

Fig.3: Full-scale ship exterior & interior layouts in each deck

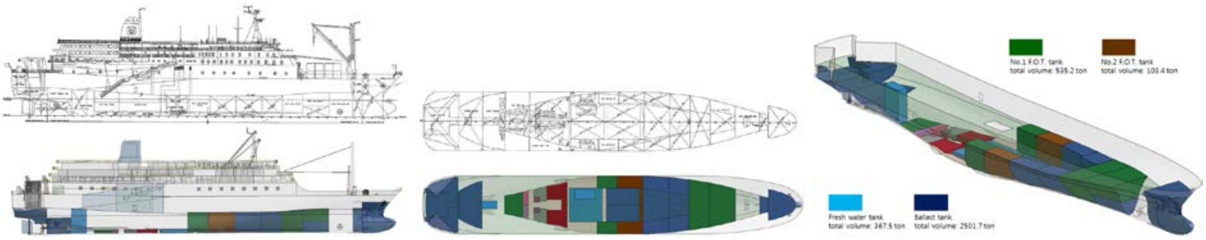

(a) side view (b) top view (c) iso view

Fig.4: Tank layout modeling in light loading condition: displacement 6,113.03ton, F.P. & A.P. draft 1.37 & 7.06m

Table 1 summarizes the hydrostatic characteristics in corrected light loading condition. In complete stability loading condition, displacement and light weight were increased by 239ton and 187ton, respectively, and center of gravity, by 0.51m, after extension and rebuilding of stern part, and removal and rebuilding of side ramp in starboard stem part. Sign error was found in the inclining test, and light weight was increased by 62.97ton, center of gravity(VCG), by 0.053m, and LCG was moved by 0.313m. Around 37ton marble was reflected in the exhibition room at A deck, after the 1st regular inspection. The final light weight was increased by around 100ton, VCG, by 0.128m, and LCG, around 0.492m.

Table 1: Hydrostatic characteristics in corrected light loading condition

Light loading condition	Weight (ton)	LCG (m)	VCG (m)
Complete stability calculation	6,113.030	-12.867	11.777
Correction of sign error in inclining test(KRISO)	6,176.000	-13.180 (-0.313)	11.830
Addition of marble slab mass in exhibition	6,213.000	-13.359 (-0.492)	11.905

Figure 5 illustrates the results of floating simulation and hydrostatic characteristic program for the light loading conditions before correction and after one, and Table 2 summarizes their fore and aft drafts and hydrostatic characteristics compared with those of stability calculations. It could be found that full-scale ship modeling in the light loading condition showed the accuracy in the error range within 0.71%.

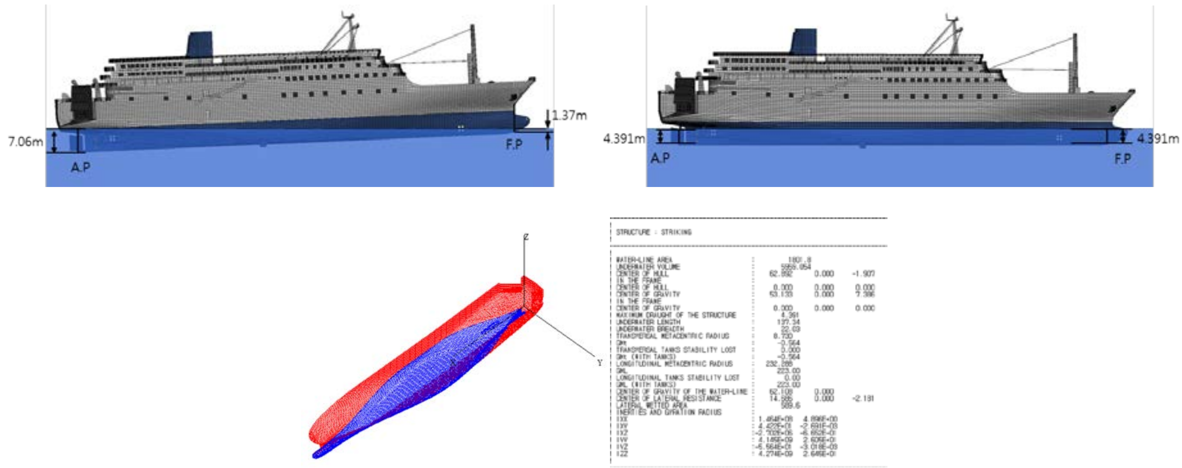

(a) before correction

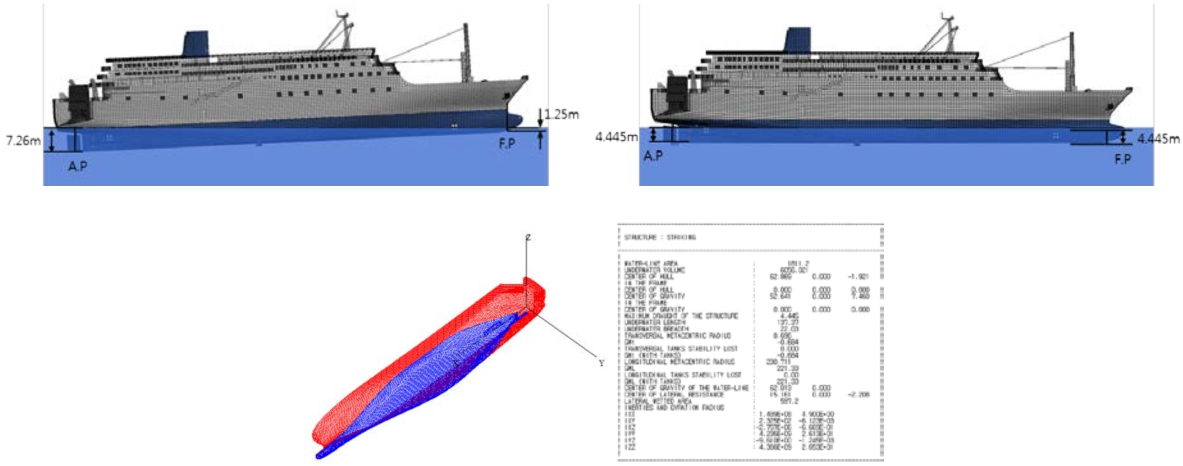

(b) after final correction

Fig.5: Floating simulation and hydrostatic characteristic program calculation for light loading condition

Table 2: Comparison of hydrostatic characteristics in light loading condition with floating simulation

item	stability calculation before correction	floating simulation	error	stability calculation after correction	floating simulation	error
displacement (ton)	6,113.03	6,108.03	-5.000(-0.08%)	6,213.000	6,207.422	-5.578(-0.09%)
volume (m^3)	5,963.930	5,959.054	-4.876(-0.08%)	6,061.463	6,056.021	-5.442(-0.09%)
LCG (from AP)	53.130	53.130	0.000(0.00%)	52.641	52.641	0.000(0.00%)
GM (m)	-0.559	-0.564	-0.004(0.71%)		-0.684	
KM (m)	11.218	11.214	-0.004(-0.03%)		11.220	
draft at LCF (m)	4.391			4.445		

4 Estimation and Modeling of Loading Condition at Accident

The estimation of loading condition at the capsize accident of ferry ship is very important factor for the analysis process of its capsizing, flooding and sinking accident. The quantity, layout and weight of shipping cargos and vehicles were predicted, through the investigation of CCTV of inboard and Incheon harbor, and the inspection of the materials of Joint Investigation Headquarters to the shippers, etc. The distribution and capacity of ballast, fuel oil and fresh water at the departure of Incheon harbor and the accident were also estimated considering the loading condition of ship handling simulation scenario Case 1 of KRISO report and the KMST report.

The quantity and layout of shipping cargos and vehicles were predicted, investigating the CCTV of inboard and Incheon harbor, as shown in Fig. 6, and inspecting the materials of Joint Investigation Headquarters to the shippers, etc. Table 3 summarizes the estimation of the quantity and weight of shipping vehicles and cargos at each deck, and the final locations of shipping vehicles and cargos at each deck are shown in Fig. 7, where the parts of red area are the vehicles with no grasp of final location through CCTV and photographs, but could be predicted by the loading paths. Figure 8 shows their layout modeling at each deck.

(a) Incheon harbor (b) inboard of ship

Fig.6: CCTV channel position of Incheon harbor and inboard of ship

Table 3: Type, quantity and weight of shipping cargos of final estimation at each deck

deck	cargo weight(ton)	Item	quantity	weight (ton)	deck	cargo weight(ton)	item	quantity	weight (ton)
Tween	42.530	sedan car	24	33.740	D	1,137.285	steel materials	2	270.000
		RV	1	1.420			trailer	3	150.000
		small car	8	7.370			empty trailer	1	5.200
C	794.560	container	45	202.500			5 ton truck	15	272.510
		steel materials	1	135.000			2.5 ton truck	1	3.000
		pipe & chassis	-	27.795			1 ton truck	4	7.745
		H-beam	-	54.000			Sedan	1	1.500
		1.0 ton truck	18	43.095			excavator	2	11.400
		2.5 ton truck	1	3.275			forklift	1	4.070
		5.0 ton truck	12	171.410			RV	22	46.000
		sedan car	31	47.370			18 ton truck	1	41.560
		RV	23	45.145			small	3	2.800
		small car	10	10.870	E	311.730	container	30	123.000
		excavator	1	13.100			bag (type 1)	20	115.900
		wreck car	1	41.000			bag (type 2)	4	11.600
D	1,137.285	woods	1	61.300			miscellaneous goods	-	25.245
		miscellaneous goods	-	113.000			wood	2	29.000
		stone & tile	10	115.700			stone & tile	-	6.985
		container	7	31.500	total	2,286.105			

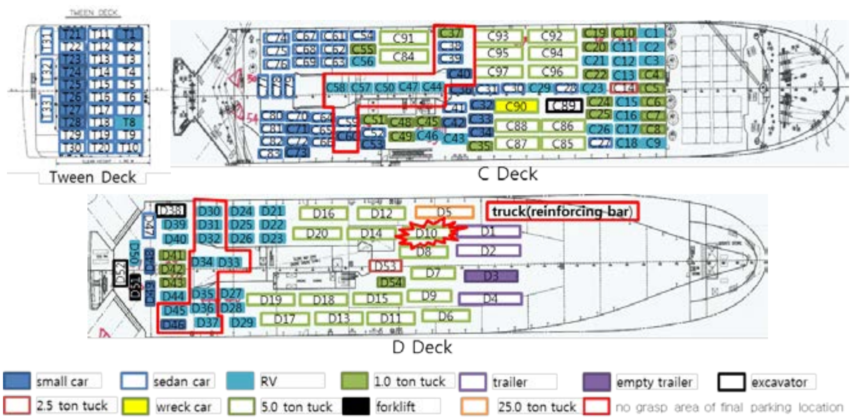

(a) vehicles at each deck

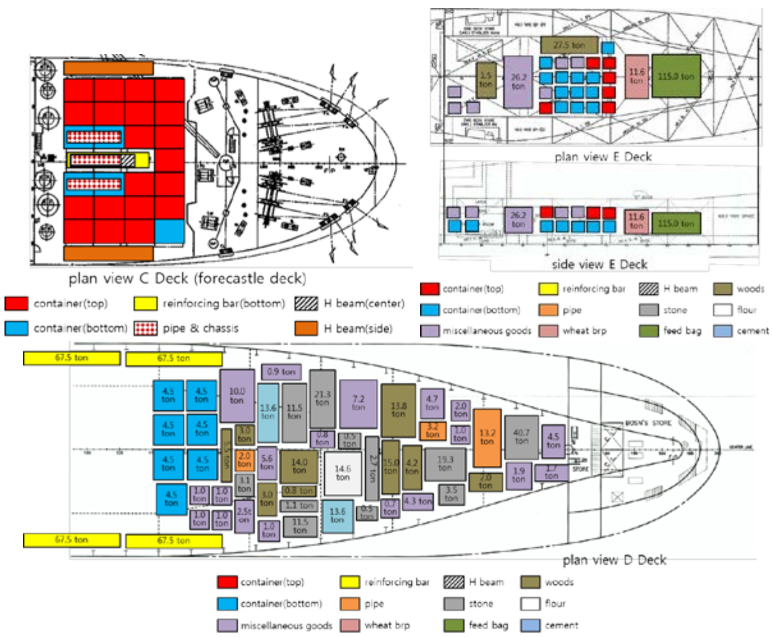

(b) cargos at each deck

Fig.7: Final locations of shipping vehicles and cargos at each deck by analysis of CCTV

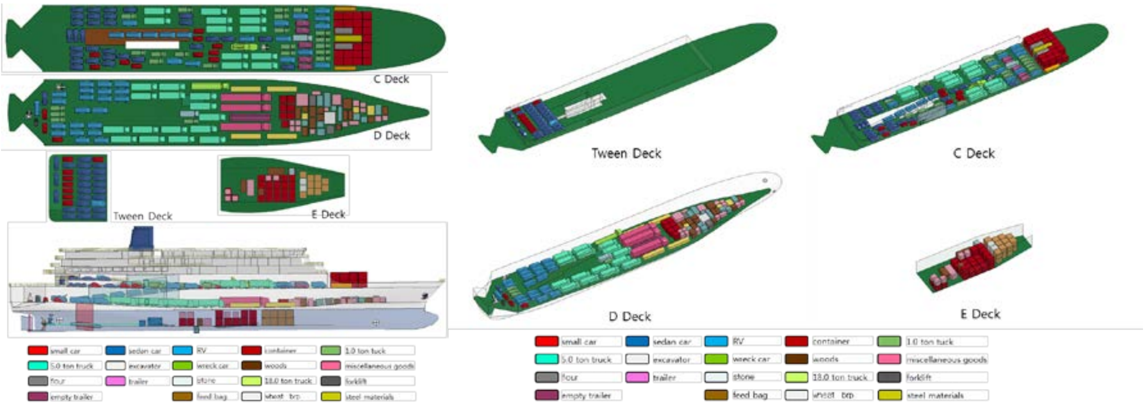

Fig.8: Vehicle and cargo layout modeling at each deck

Table 4 summarizes the estimation of loading condition of ballast, fuel oil and fresh water at accident according to tank in detail, referring to the reports of KRISO and KMST, and the statements of the 1st mate and chief engineer, where 3% of natural loss weight of ballast tank No. 2, 4 & 5 of KMST report was applied to the distribution and weight estimation. The final estimation of loading condition of ballast, fuel oil and fresh water at accident was modeled, as shown in Fig. 9, and loading weight and its ratio according to tank is shown in Fig. 10.

Table 4: Comparison of loading condition of ballast, fuel oil and fresh water at accident

loading condition at accident		KRISO report Case 1 (ton)	KMST report(natural loss) (ton)		modeling (ton)
			non-reflection	reflection	
Ballast Water	FPT (C)	0.000	0.000	0.000	0.000
	No.1 B.W.T (C)	82.000	82.000	82.000	82.000
	No.2 B.W.T (C)	206.300	206.310	200.121	200.121
	No.3 B.W.T (P/S)	0.000	0.000	0.000	0.000
	No.4 B.W.T (C)	147.500	147.506	143.081	143.081
	No.5 B.W.T (P)	110.900	110.864	107.538	107.538
	No.5 B.W.T (S)	111.900	111.992	108.632	108.632
	No.6 B.W.T (S)	0.000	0.000	0.000	0.000
	APT (C)	0.000	0.000	0.000	0.000
	Heel Tank (P/S)	102.600	102.600	102.600	102.600
	Ballast Water Total	761.200	761.272	743.972	743.972
Fuel Oil	No.1 F.O.T (P) : C oil	49.400			49.400
	No.1 F.O.T (S) : C oil	49.400			49.400
	No.2 F.O.T (P) : A oil	14.800			14.800
	No.2 F.O.T (S) : A oil	14.800			14.800
	Fuel Oil Total	128.400	128.380	128.380	128.400
Fresh Water	No.1 F.W.T (P)	22.500			22.500
	No.1 F.W.T (S)	22.500			22.500
	No.2 F.W.T (C)	147.000			147.000
	Fresh Water Total	192.000	192.000	192.000	192.000

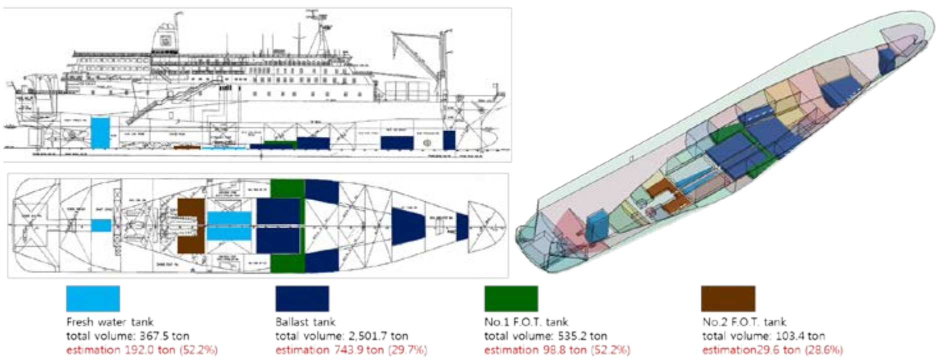

Fig.9: Distribution modeling of ballast, fuel oil and fresh water in each deck at accident

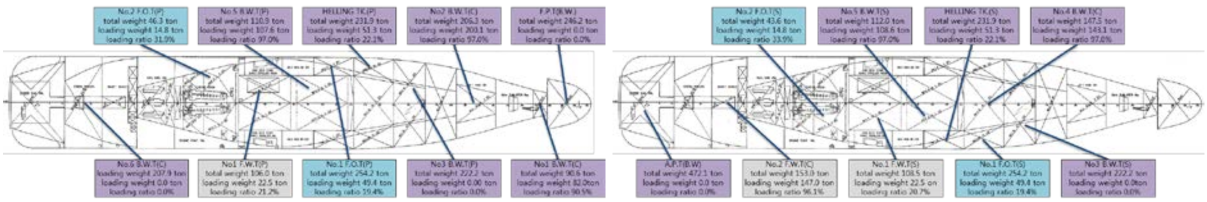

(a) port (b) starboard

Fig.10: Loading weight distribution and ratio in each deck at accident

Table 5 shows the comparison of loading conditions and the final estimation at accident, where the free surface effect of 3% of natural loss weight of ballast tank No. 2, 4 & 5 of KMST report was not considered in GoM calculation because of very small effect. As shown in Fig. 11, floating simulation and hydrostatic characteristic program calculation were carried out according to loading condition of cargo, ballast, fuel oil and fresh water at accident, and its hydrostatic characteristics, such as fore and aft drafts, GoM, are shown in Table 5.

Table 5: Comparison of loading condition and estimation at accident

loading condition at accident		weight (ton)			
		KRISO report Case 1	KMST report(natural loss)		modeling
			non-reflection	reflection	
Passenger/ Crew	Navigation Bridge Deck	3.500	3.500	3.500	3.500
	A Deck	33.700	33.700	33.700	33.700
	B Deck	5.600	5.600	5.600	5.600
	Total	42.800	42.800	42.800	42.800
Cargo	Tween Deck	35.500	35.500	35.500	42.500
	C Deck	924.500	911.100	911.100	794.500
	D Deck	742.000	762.00	762.000	1137.400
	E Deck	440.700			311.700
	Cargo Total	2,142.700	2,142.700	2,142.700	2,286.100
Ballast Water	Ballast Water Total	761.200	761.200	743.972	743.972
Fuel Oil	Fuel Oil Total	128.400	128.380	128.380	128.400
Fresh Water	Fresh Water Total	192.000	192.000	192.000	192.000
Provision	-	0.700	0.700	0.700	0.700
Lubrication	-	0.000			
DWT Constant	-	166.200	166.200	166.200	166.200
Dead Weight	-	3,434.000	3,433.980	3,416.752	3,560.172
Light Weight	-	6,176.000	6,213.000	6,213.000	6,213.000
Displacement	-	9,610.000	9,646.980	9,629.752	9,773.172
sailing state (m)					
draft at F.P.		5.718	5.552	5.526	5.695
draft at A.P.		6.435	6.063	6.053	6.578
Trim		-0.717	-1.022	-1.054	-0.883
GM	-	0.700	0.730	0.730	0.589
GGo	-	-0.110	0.120	0.350	0.114
GoM	-	0.590	0.620	0.380	0.475

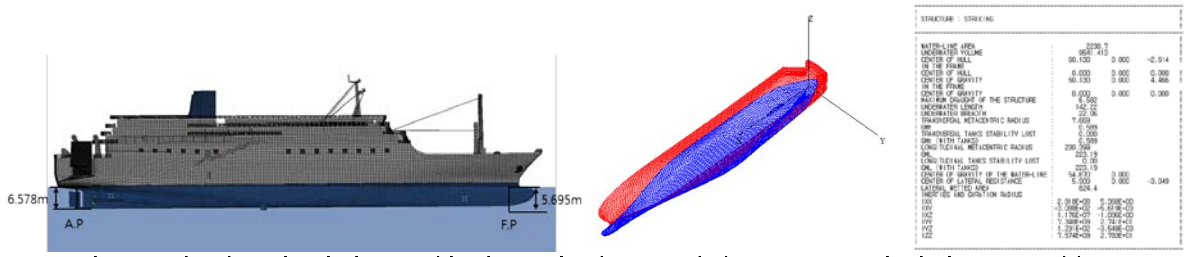

Fig.11: Floating simulation and hydrostatic characteristic program calculation at accident

It is reasonable to consider the slip of cargos on the deck due to poor lashing among the major capsize factors during rapid turning as the worsening of the lateral heel angle of the ship with weak stability in addition to the centrifugal force during truning. In this study, inclining simulation was carried out for the friction coefficient and lashing of cargo and vehicle affecting the cargo shifting, and cargo and vehicle modeling was modified comparing with those of experiments carried out by Korea Transportation Safety Authority(TS) and National Forensic Service(NFS).

Inclining test of sedan, RV, heavy truck and construction equipment with tires were carried by TS using slip plate in the case of no lashing, single side lashing and both side lashing, as shown in Table 6. Friction measuring test of 1.0 ton truck, container and plastic pallet with miscellaneous goods was also performed by NFS in the decks of MV Ohamana similar to the accident ferry ship. It was reported that the maximum static friction coefficient 0.69 was measured for 1.0 ton truck in C deck, and the other friction ones of container and pallet could not be standardized because of test place of D deck with bumped surface of crossed short reinforcing bars.

Table 6: Slip starting angle according to vehicle (TS)

vehicle type	vehicle name	weight (ton)	slip starting angle (°)		
			no lashing	single side lashing	both side lashing
Sedan	EF Sonata	1.36	29.7	31.0	32.5
RV	Sorento R	1.82	29.1	28.2	30.6
heavy truck	5 ton tank lorry	5.97	25.2	24.7	25.0
construction equipment	skid loader	4.00	26.7	-	-
	wheel loader	31.00	26.0	-	-

The trend between the slip starting angle and weight of vehicles with tires was checked in the case of no lashing in Table 6, as shown in Fig. 12. Since the weight per slip starting angle is proportional to the weight, any vehicle with tires could be estimated by this trend, and Table 7 summarized the estimated slip starting angle for the several vehicles in the case of no lashing. Slip starting angles of container and pallet were adopted as 0.4 and 0.3, respectively, as the report of KRISO.

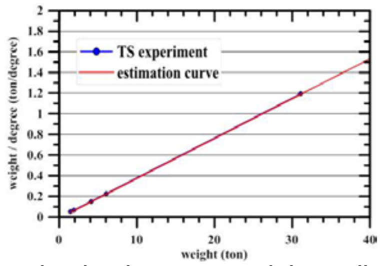

Fig.12: Floating between weight & slip angle

Table 7: Slip starting angle according to vehicle(no lashing)

vehicle type	weight (ton)	slip starting angle (°)
Sedan	1.5	29.2
RV	2.0	28.3
1.0 ton truck	2.5	27.8
5.0 ton truck	14.0	26.2
trailor	40.0	26.0

Inclining simulation was carried for the vehicles with tire in Table 7, and container and pallet with steel and miscellaneous goods, and their slip starting angle response behavior according to slope angle is shown in Fig. 13 and summarized in Table 8. According to the inboard CCTV and photos, and statements of lashing agency, the general lashing was very poor, the maximum lashing of vehicle under 4.5 ton was both sides, and that of vehicle beyond, 4 sides, with very old lashing bands and gears. There was no reasonable lashing at the container and pallet cargo with bottom and top position. The slip of these container and pallet cargos were affected by the bump of deck floor and its wetness. These conditions are summarized in Table 7. Figures 14 and 15 show the slip starting angle response behavior of vehicle with lashings according to slope angle, and that of turnovered vehicle, respectively. Friction coefficient by the lashing was accounted to that of slip by the equivalent friction one.

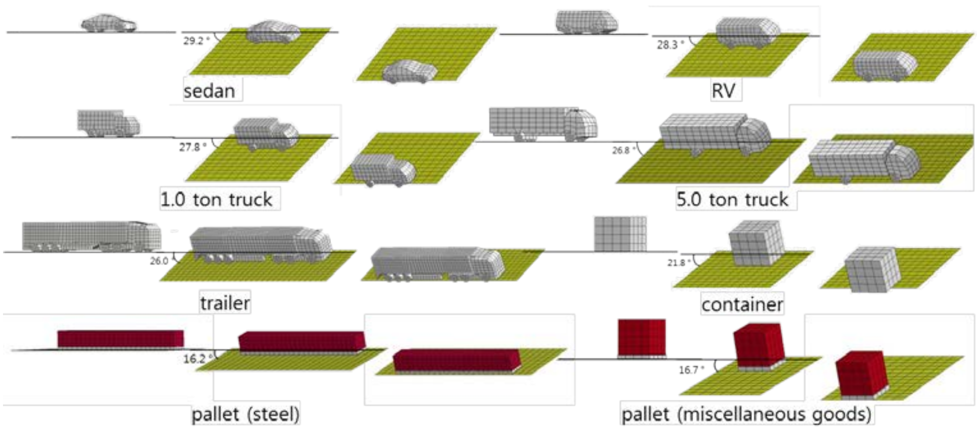

Fig.13: Slip starting angle behavior of vehicle and cargo without lashing according to slope angle

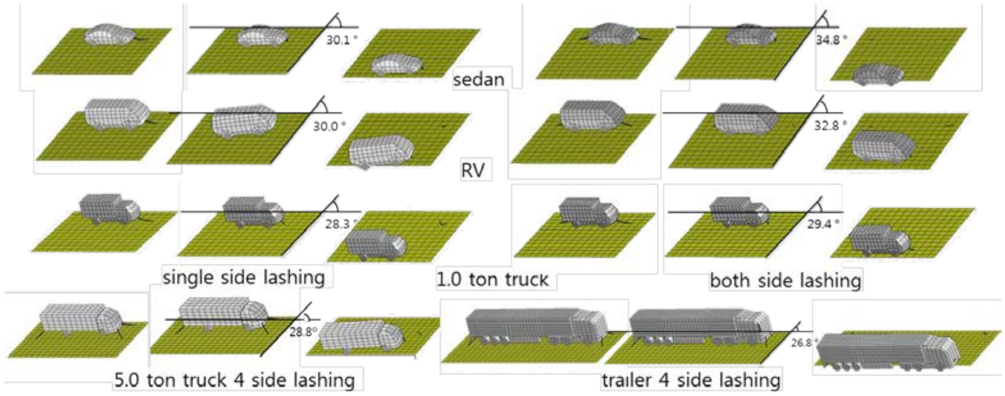

Fig.14: Slip starting angle behavior of vehicle with lashing according to slope angle

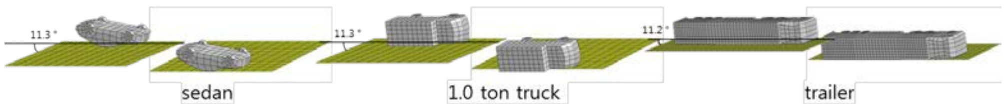

Fig.15: Slip starting angle behavior of turnovered vehicle without lashing according to slope angle

Table 8: Slip starting angle and equivalent friction coefficient according to vehicle and cargo

		C Deck		D Deck		E Deck	
	lashing	slip angle(°)	equi. friction coeff.	slip angle(°)	equi. friction coeff.	slip angle(°)	equi. friction coeff.
sedan	-	29.2	0.56	31.2	0.60	-	-
	1 side	30.1	0.57	32.1	0.62	-	-
	2 side	34.8	0.69	36.8	0.75	-	-
	turnover	11.3	0.20	11.3	0.20	-	-
RV	-	28.3	0.54	30.3	0.58	-	-
	1 side	30.0	0.58	32.0	0.62	-	-
	2 side	32.8	0.64	34.8	0.70	-	-
	turnover	11.3	0.20	11.3	0.20	-	-
1.0 ton truck	-	27.8	0.53	29.8	0.57	-	-
	1 side	28.3	0.54	30.3	0.58	-	-
	2 side	29.4	0.56	31.3	0.61	-	-
	turnover	11.3	0.20	11.3	0.20	-	-
5.0 ton truck	4 side	28.8	0.55	30.7	0.59	-	-
	turnover	11.2	0.20	11.2	0.20	-	-
trailor	4 side	-	-	28.8	0.55	-	-
	turnover	-	-	11.2	0.20	-	-
container (bottom)	-	21.8	0.40	26.8	0.50	16.7	0.30
container (top)	-	11.3	0.20	-	-	11.3	0.20
pallet(steel)	-	16.2	0.30	21.3	0.40	-	-
pallet(misc. goods)	-	16.7	0.30	21.8	0.40	11.3	0.20
pallet(top)	-	11.3	0.20	-	-	11.3	0.20

5 Full-Scale Ship Turning Simulation

Full-scale rapid turning simulation was carried out for the investigation of capsize accident cause of ferry ship, according to the rudder angle, ship velocity, GoM, and lashing at the accident, using MAIAS(highly advanced M&S system of FSI analysis technology), and comparing its simulation results with the real AIS track and heeling angle. MAIAS was verified through the full-scale ship turning simulation by comparison with maneuvering performance sea trial test result of initial building ship.

Figure 16 shows the maneuvering performance sea trial test report, record and its track of its initial building ship. This shows the 360 degree port & starboard turning track at 23.23 knots full speed with twin propeller and single rudder, and ferry ship was initially inclined to the 1.0 degree to the port side, and the maximum longitudinal and transverse distances were 475 and 563 m, respectively. In this study, twin propeller hard starboard turning simulation was carried out, where ferry ship was floating by the hydrostatic characteristics program and floating simulation by the fore and aft drafts, as shown in Fig. 17. Turning simulation was verified using Fluid-Structure Interaction analysis technique through the comparison of sea trial test report.

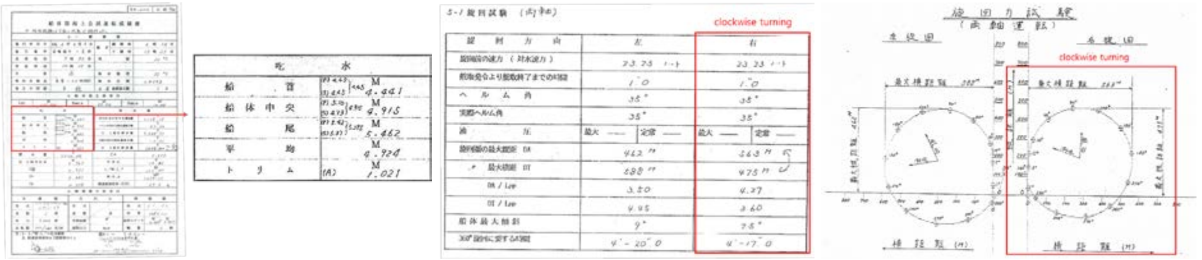

(a) sea trial test report (b) sea trial test record (c) sea trial port & starboard turning track

Fig.16: Sea trial test report, record and its track of ferry ship

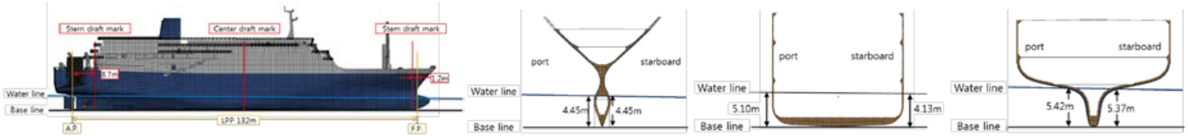

Fig.17: Sea trial test model with port and starboard draft at stem, center and stern sections

Figure 18 shows the full-scale fluid modeling and its dimensions for the starboard turning simulation using MAIAS, and Fig. 19, full-scale sea trial starboard turning test simulation behavior and its comparison with test track, respectively. It could be found that full-scale sea trial starboard turning test response was agreed relatively very well with test track, and MAIAS could be suitable for the rapid turning simulation of ferry ship capsize accident.

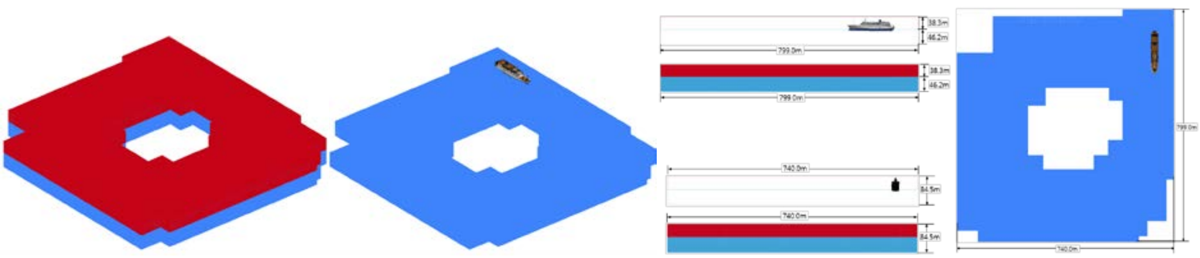

Fig.18: Full-scale fluid modeling and its dimensions for sea trial test turning simulation

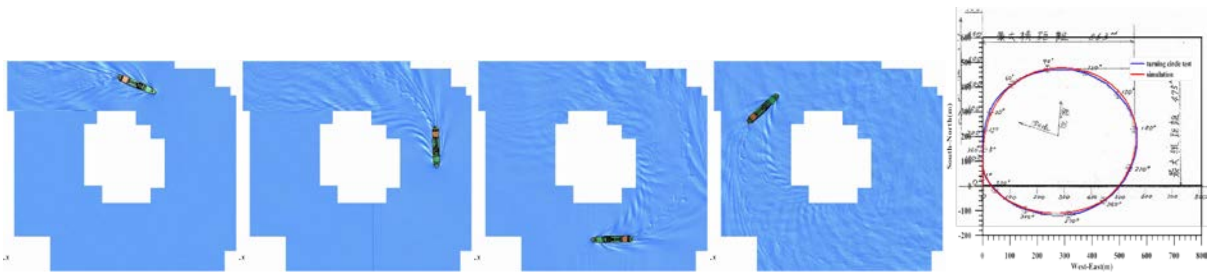

Fig.19: Full-scale sea trial starboard turning test simulation behaviorand its comparison with track

Figure 20 shows the AIS track of rapid turning for ferry ship capsize and sinking accident, and heading angle was revised by the MNMU[7]. Full-scale rapid turning simulation was carried out for the investigation of capsize accident situation according to the rudder angle, ship velocity, GoM, and lashing at the accident, using MAIAS. Through the close investigation of CCTV and inspection of the materials of Joint Investigation Headquarters to the shippers, the weight and layout of shipping cargos and vehicles were predicted for the exact GoM 0.475m, as shown in Table 9. Two more GoM's, 0.359m and 0.590m, were considered for more exact investigation of capsize accident cause, where the former was the applied weighting to the cargos and vehicles except empty vehicles(new and rent cars) for the consideration of excessive shipping, as shown in Table 10 and Fig. 21(a), and the latter, the Case 1 of KRISO report, as shown in Fig. 21(b).

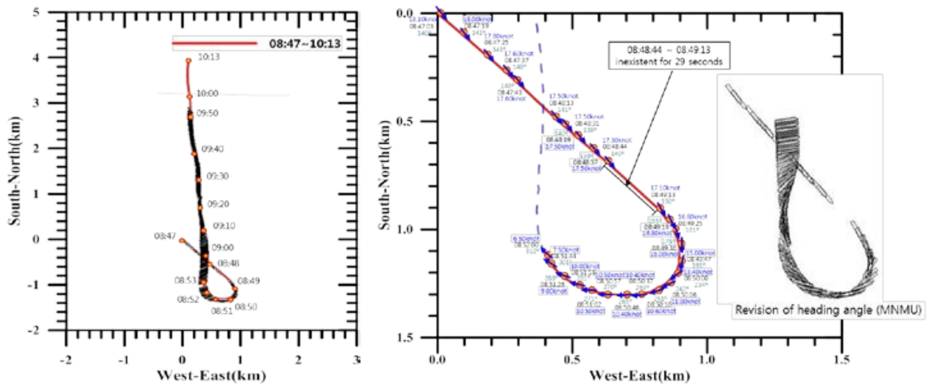

(a) over view (b) close view

Fig.20: AIS track of rapid turning of ferry ship capsize and sinking accident

Table 9: Comparison of loading condition for rapid turning simulation

		weight (ton)		
		modeling	weighting	KRISO
Passenger/Crew	Navigation Bridge Deck	3.500	3.500	3.500
	A Deck	33.700	33.700	33.700
	B Deck	5.600	5.600	5.600
	Total	42.800	42.800	42.800
Cargo	Tween Deck	42.500	43.991	35.500
	C Deck	794.500	840.167	924.500
	D Deck	1,137.400	1,190.421	742.000
	E Deck	311.700	316.314	440.700
	Cargo Total	2,286.100	2,390.893	2,142.700
Ballast Water		743.972	743.972	761.200
Fuel Oil	Fuel Oil Total	128.400	128.400	128.400
Fresh Water	Fresh Water Total	192.000	192.000	192.000
Provision	-	0.700	0.700	0.700
DWT Constant	-	166.200	166.200	166.200
Dead Weight	-	3,560.172	3,664.965	3,434.000
Light Weight	-	6,213.000	6,213.000	6,176.000
Displacement	-	9,773.172	9,877.965	9,610.000
sailing state (m)				
draft at FP	-	5.695	5.951	5.718
draft at AP	-	6.578	6.474	6.435
Trim	-	-0.883	-0.523	-0.717
GM	-	0.589	0.473	0.700
GGo	-	0.114	0.114	0.110
GoM	-	0.475	0.359	0.590

Table 10: Loading condition with weighting for rapid turning simulation

	modeling	weighting
vehicle under 5.0 ton	-	15% (exemption of empty one)
vehicle beyond 5.0 ton	-	10% (99.8 ton)
container	78 ea (4.500 ton/ea)	78 containers (4.650 ton/ea)
	4 ea empty (1.500 ton/ea)	4 ea empty (1.670 ton/ea)
displacement	9,773.172 ton	9,877.965 ton
Trim	-0.883 m	-0.523 m
GoM	0.475 m	0.359 m

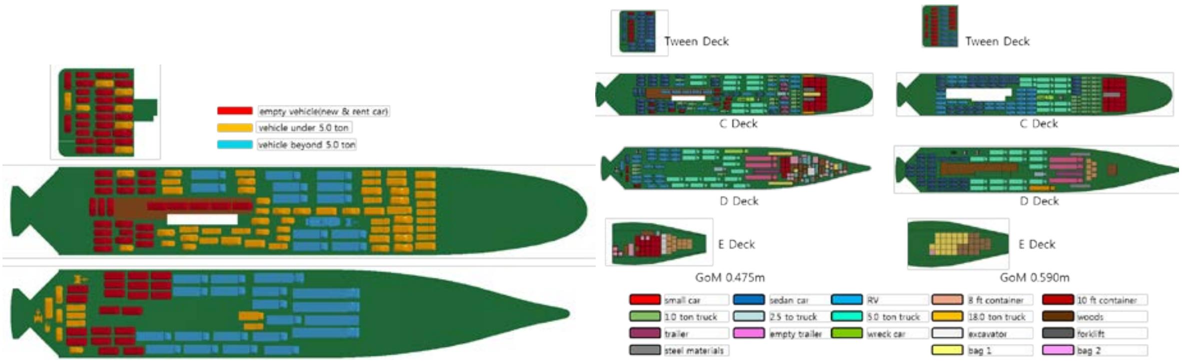

(a) weighting vehicle & cargo (b) layouts between GoM 0.475m & 0.590m

Fig.21: Loading condition of weighting, comparison of layout of GoM 0.475m & 0.590m

Figure 22 shows the full-scale fluid modeling and its dimensions for the rapid turning simulation using MAIAS. Rapid turning simulation was carried out by the scenarios, as shown in Table 11, for three GoM, 0.359m, 0.475m and 0.59m. Figure 23 shows the full-scale rapid turning simulation behavior of each scenario with AIS track at accident, and Fig. 23, close view of simulation behavior of Case 2-2. Figure 24 shows all full-scale rapid turning simulation behaviors together with AIS track, and lateral heel angle responses of all scenarios. It could be found that full-scale sea trial starboard turning test response was agreed relatively very well with test track, and MAIAS could be suitable for the rapid turning simulation of ferry ship capsize accident.

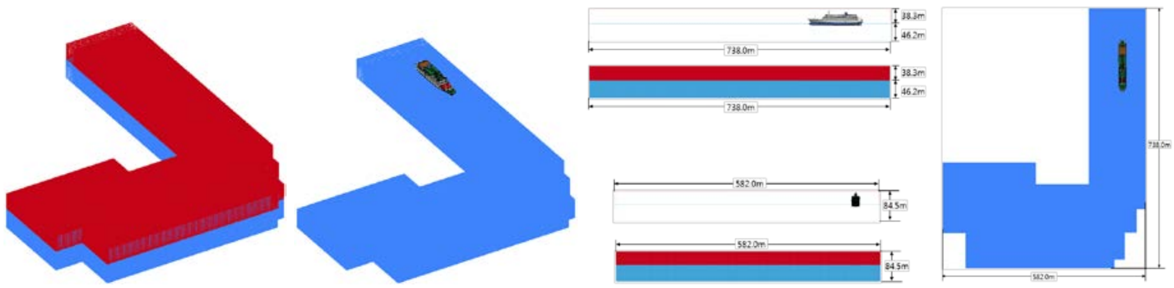

Fig.22: Full-scale fluid modeling and its dimensions for rapid turning simulation

Table 11: Scenario of full-scale rapid turning simulation

Case		GoM (m)	ship velocity (knots)	rudder angle (°)	rudder restoration	cargo shift
Case 1	Case 1-1	0.359	17.1	35	maintenance	shift
	Case 1-2				restoration	
Case 2	Case 2-1	0.475	17.1	35	maintenance	shift
	Case 2-2				restoration	
	Case 2-3					fixed
	Case 2-4			20		shift
Case 3	Case 3-1	0.590	17.1	35	restoration	shift
Case 4	Case 4-1	0.475	19.0	35	restoration	shift

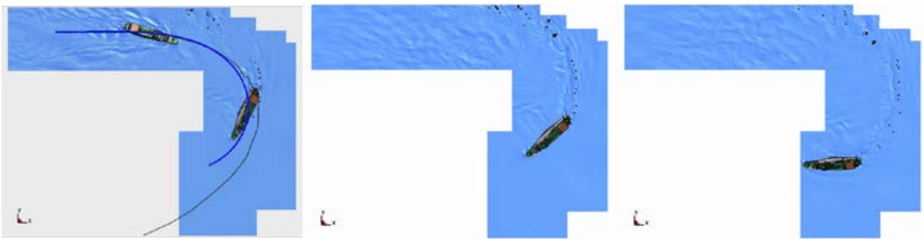

(a) Case 1-1

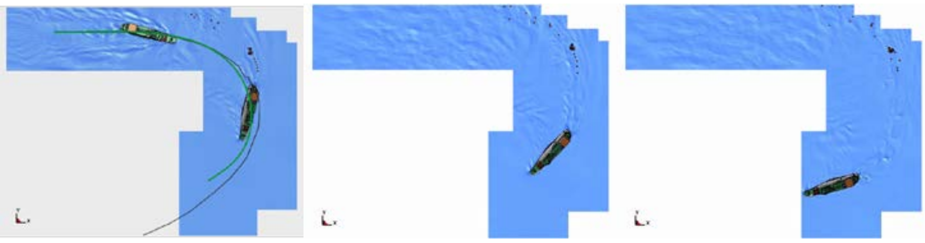

(b) Case 1-2

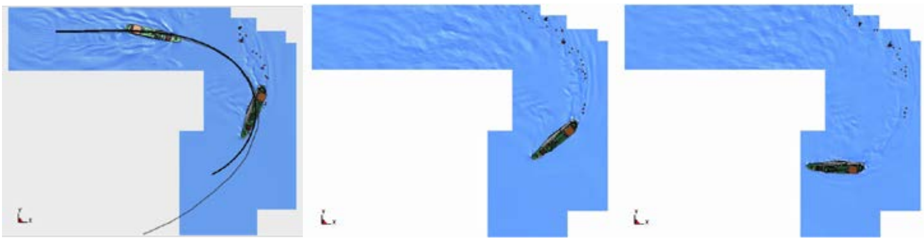

(c) Case 2-1

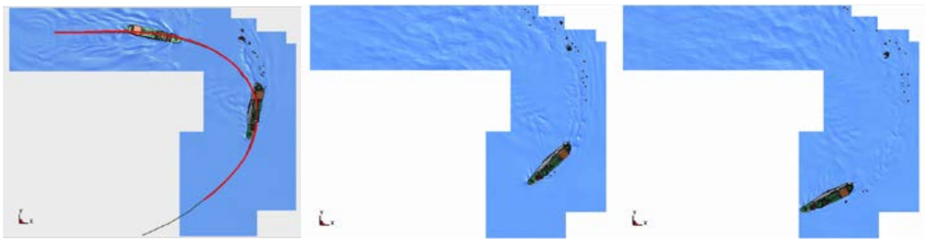

(d) Case 2-2

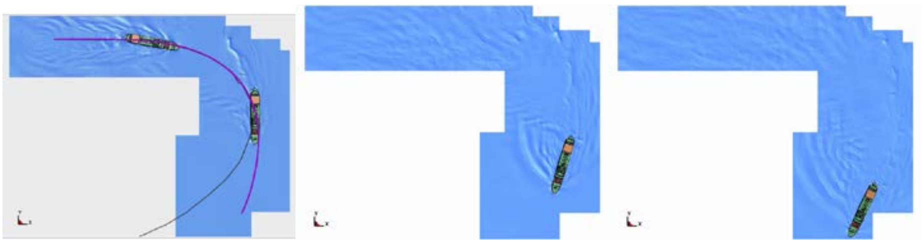

(e) Case 2-3

(f) Case 2-4

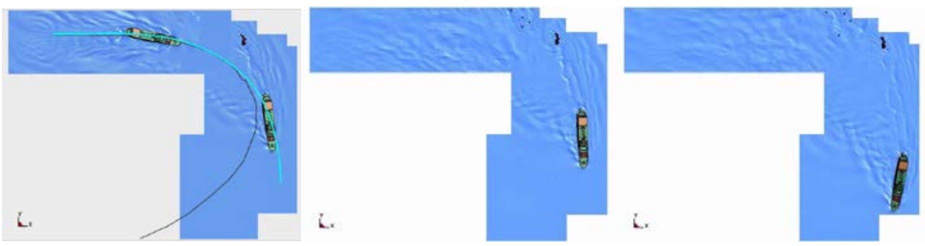

(g) Case 3-1

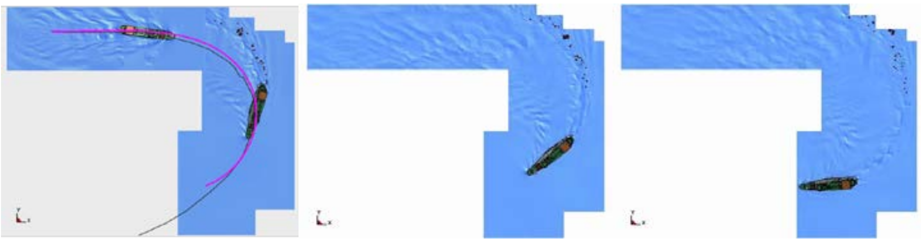

(h) Case 4-1

Fig.23: Full-scale rapid turning simulation behavior according to scenario in top view

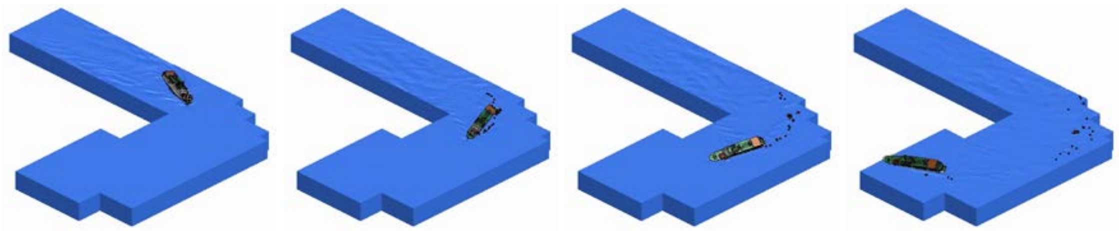

(a) iso view

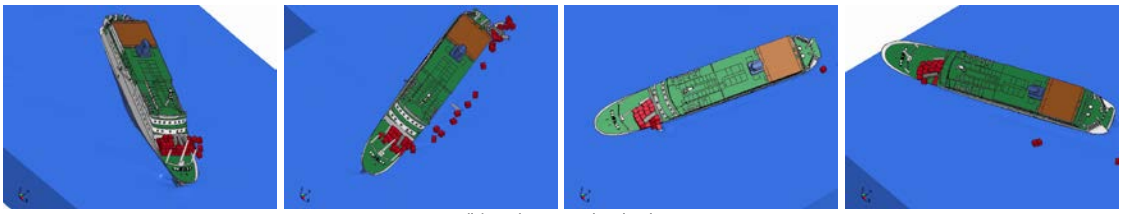

(b) C forecastle deck

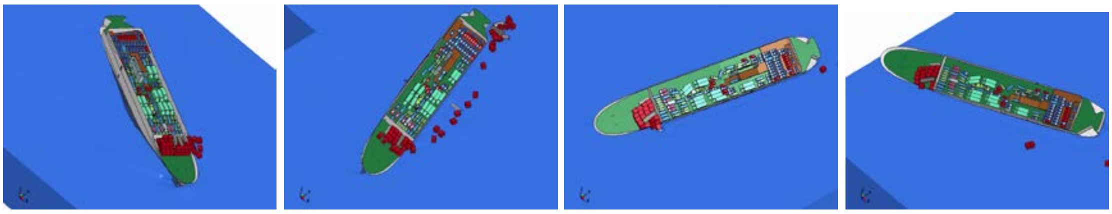

(c) C deck

(d) D deck

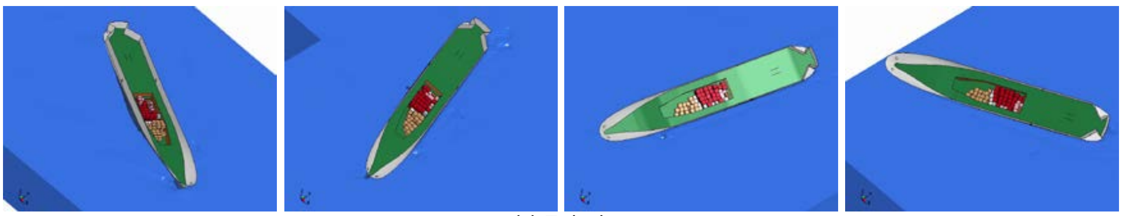

(e) E deck

Fig.24: Full-scale rapid turning simulation behavior in Case 2-2 in close view

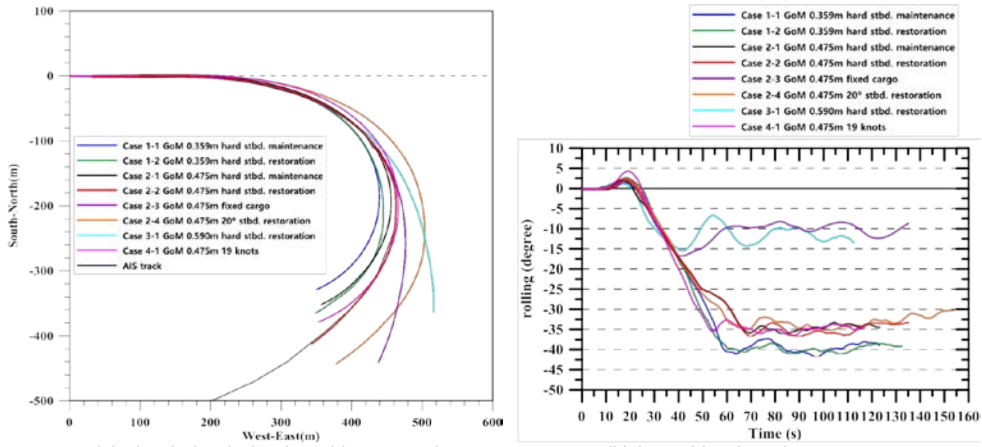

(a) simulation behavior with AIS track (b) lateral heel angle response

Fig.25: Full-scale rapid turning simulation behavior with AIS track & lateral heeling angle response

From the full-scale ship rapid turning simulation behavior and AIS track, and lateral heel angle response, it could be confirmed that those of Case 2-2 were close to the AIS track and to the lateral heel angle 35 degree at real capsize accident. It could be estimated that the predicted weight and layout of vehicle and cargo at each deck were also agreed to the capsize accident situation. Cargos including containers on the C forecastle deck were poured into the sea water, and all cargos at each deck were also shifted to the port side at each deck, when excessive outward heel occurred.

In the case of no rudder restoration of Case 2-1, ferry ship was turned rapidly inward of AIS track as expected, and in the case of very good lashing of Case 2-3, around 15 degree of lateral heel angle took place and was turned outward of AIS track. In the case of 20 degree rudder angle, not the hard starboard, of case 2-4, lateral heel angle occurred as the case of 35 degree one, but the ship was turned outward of AIS track at initial stage. From this outward turning track, it could be considered that ferry ship was turned rapidly with hard starboard, and could be capsized at 20 degree rudder angle in the case of poor lashing. Around 19.0 knots of ship velocity a little bit larger than 17.1 knots in Case 4-1 did not make the large outward of AIS track unexpectedly, and made inward of AIS track after initial rapid turning and almost the same lateral heel angle.

In the case of the consideration of a little bit large weighting with GoM 0.359m in Case 1, quick turning occurred more inward of AIS track, as expected, and around 40 degree lateral heel angle also occurred. From these responses, it could be confirmed that estimation of weight and distribution of vehicle and cargo at each deck from the close investigation of CCTV and inspection of shippers was almost closer to the real accident situations. In the case of GoM 0.590m of KRISO in Case 3-1, around 15 degree lateral heel angle occurred as the case of good lashing condition, only top cargos on C forecastle and E decks were poured and most of them were not moved, and quick turning happened greatly large outward of AIS track.

6 Considerations

Through this study, it could be confirmed that the weight and layout of vehicle and cargo was estimated relatively very well at the capsize accident, and that full-scale ship turning and rapid turning simulation was very close to the sea trial turning test and AIS track using MAIAS (highly advanced M&S system of Fluid-Structure Interaction analysis technique). It could be considered that reasonable weight and distribution on deck should be loaded on the ship for the good stability, but, above all things, lashing should be carried out according to the rules against cargo shift or leaning.

7 Acknowledgement

This research was performed by the support of Special Investigation Commission on 4/16 Sewol Ferry Disaster. The authors would like to express our appreciation to their supports.

8 Literature

[1] LSTC, LS-DYNA User's Manual, Version 971 R7, Livermore Soft Technology Corp., USA, (2013).

[2] Aquelet, N., Souli, M., and Olovsson, L., Euler–Lagrange coupling with damping effects: Application to slamming problems, Computer Methods in Applied Mechanics and Engineering, 195, (2006), 110–132.

[3] Souli, M., Ouahsine, A., and Lewin, L., ALE formulation for fluid-structure interaction problems, Computer Methods in Applied Mechanics and Engineering, 190, (2000), 659-675.

[4] Joint Investigation Headquarters, Cause Investigation of Ferry SewolSinking Accident, Final Report, (2014).

[5] KRISO, Cause Investigation of Sewol Sinking Accident, Final Report, (2014).

[6] KMST, Special Investigation of Ferry Sewol Capsize Accident, Final Report, (2014).

[7] Im, N.K., AIS Data Simulation and Analysis of Ferry Sewol Navigation Characteristics, Final Report, (2015).